Protonation of Lysozymes and Its Consequences for the Adsorption onto a Mica Surface

ARTICLE *in* LANGMUIR · JULY 2012

Impact Factor: 4.46 · DOI: 10.1021/la301558u · Source: PubMed

3 AUTHORS, INCLUDING:

Barbara Jachimska
Polish Academy of Sciences
38 PUBLICATIONS **623** CITATIONS
SEE PROFILE

Anna Pajor-Świerzy
Instytut Katalizy i Fizykochemii Powierzchni i…
5 PUBLICATIONS **38** CITATIONS
SEE PROFILE

Langmuir

Article

pubs.acs.org/Langmuir

Protonation of Lysozymes and Its Consequences for the Adsorption onto a Mica Surface

B. Jachimska,* A. Kozłowska, and A. Pajor-Świerzy

J. Haber Institute of Catalysis and Surface Chemistry, Polish Academy of Sciences (PAS), Niezapominajek 8, 30-239 Cracow, Poland

ABSTRACT: Several physicochemical properties of chicken egg white lysozyme (LSZ) in electrolyte solutions were determined. The hydrodynamic diameter of LSZ at an ionic strength of 0.15 M was found to be 4.0 nm. Using the determined parameters, the number of uncompensated (electrokinetic) charges, N_c, on the molecule surface was calculated from the electrophoretic mobility data. It was found that the N_c = 2.8 at pH = 3.0 and an ionic strength of I = 0.15 M. At the lower ionic strength, $I = 1 \times 10^{-3}$ M, this positive charge increased to N_c = 5.6 at a pH = 3.0 The physicochemical characteristics were supplemented by the dynamic viscosity measurements. The intrinsic viscosity and the hydrodynamic diameter results were compared with theoretical predictions from Brenner's model. Using this approach, it was found that the effective molecule length of LSZ is equal to L_{ef} = 5.6 nm. Additional information on the LSZ adsorbed films was obtained by the contact angle measurements. The notably large contact angles were measured on LSZ films formed under the conditions where both the LSZ and the mica were oppositely charged. The higher the positive zeta potential of LSZ, the greater the contact angle measured, which indicates that LSZ affinity for the adsorption on mica increases with its uncompensated charge. The adsorption dependence on the zeta potential of LSZ was explained, assuming a roughly uniform distribution of the net charge on the molecule surface. This assumption is supported by the results of depositing negatively charged, fluorescent latex particles onto the mica surface, which had been modified by LSZ adsorption. The highest latex coverage was formed on mica surfaces that had first been coated with LSZ solutions of lower pH, as a result of the increasing charge of LSZ monolayers in this condition.

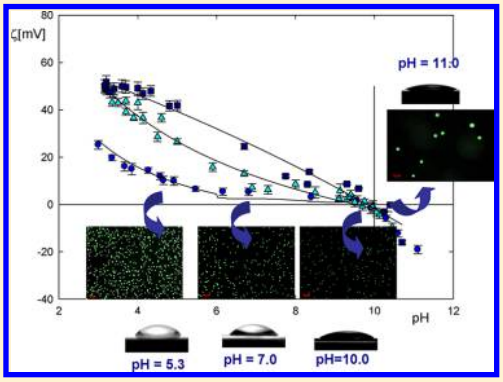

1. INTRODUCTION

The development of bionanotechnology requires nanoscale control of molecular orientation and organization, which is also essential for understanding the mechanisms of protein monolayer formation and their properties, which play a crucial role in their future applications. Despite the recent progress in protein applications, there are still required fundamental studies because the adsorption process and structure of the formed surface films are still far from being completely understood.

Lysozyme exhibits strong antibacterial activity against gram-positive bacteria. This property has found practical applications in the medicinal and pharmaceutical industries. The adsorption of lysozyme (LSZ) onto various surfaces has been widely studied using a variety of experimental techniques, including neutron reflection, total internal reflectance fluorescence (TIRF), circular dichroism (CD), streaming potential, elipsometry, and atomic force microscopy (AFM).[1−14]

It is considered that LSZ is structurally stable upon adsorption.[9] For example, reflectometry and total internal reflectance fluorescence (TIRF) techniques have shown that the LSZ does not denature upon adsorption onto negatively charged silica surfaces.[3,4] Similarly, the adsorption of LSZ onto mica does not induce any significant conformational changes, and the orientation of the molecule demonstrates a dependence on its concentration.[12] At low LSZ concentrations (0.002 mg/mL), a densely packed side-on adsorbed layer of LSZ is observed, whereas at higher concentrations (>0.002 mg/mL), end-on adsorption also occurs.

The direct imaging of LSZ adsorption onto mica was performed by Kim et al.[13] using AFM under acidic conditions with different bulk concentrations of the protein. These authors observed the formation of LSZ clusters on the mica surface and suggested diffusion of LSZ molecules along the surface. In all cases, the LSZ adsorption was found to be irreversible.

Both theoretical and experimental studies have suggested that the protein adopts a preferential orientation when adsorbed at the mica-solution interface.[3,4,7,15] Daly[4] demonstrated that two-stage reorientation occurs in the LSZ monolayer during adsorption through the use of two independent experimental techniques (TIRF and streaming current). The first stage involves orienting the LSZ with the most positively charged domain on the silica surface. In the second stage, a slow reorientation occurs while the monolayer approaches the saturation state.

Carlsson's[15] analysis demonstrates that the preferential orientation of LSZ cannot be satisfactorily explained by only the dipole moment of the protein; rather, the quadruple

Received: April 17, 2012
Revised: June 24, 2012
Published: July 11, 2012

moment should also be taken into account for explaining the preferential orientation.

The proper description and control of protein deposition require a thorough knowledge of the protein structural and transport properties, such as the molecular shape, conformational changes, degree of hydration, uncompensated charge, diffusion coefficient ,and the possible aggregation phenomena. With regards to the dependencies of these properties on the bulk concentration, electrolyte composition, ionic strength, pH, and temperature must also be considered. The surfaces of all proteins are composed of a mixture of hydrophilic and hydrophobic residues. The polar and nonpolar residues are not uniformly distributed over the protein surface. For this reason, the spatial charge distribution is often highly asymmetric, which is reflected in the protein dipole moment and, in turn, influences the adsorption and molecular orientation at the interface. The adsorption is a multistep process during which the protein can be found in many different orientation/conformational states. The first step of the adsorption of a protein onto a solid support is highly important for understanding the solid surface modification.

In our previous work, we demonstrated the large effect that the conditions under which the adsorption occurred has on the structure and properties of bovine serum albumin (BSA) monolayers on mica.[16] The interfacial properties of proteins are important for the adhesion of biological organisms, such as bacteria or cells, on the protein film.

In this work, we determined a number of molecular properties of LSZ, both in the solution bulk and at the mica−solution interface, using complementary physicochemical methods. The dynamic laser scattering (DLS) and viscosity measurements were used to characterize LSZ macromolecules in electrolyte solutions. These measurements were supplemented with electrophoretic mobility measurements, which allowed us to determine the isoelectric point and the uncompensated (electrokinetic) charge of the LSZ molecule. The results from these measurements provide insight into the dynamic structure of LSZ in the bulk solution.

In the second part of the article, we characterize the monolayer adsorption coverage of LSZ on mica surfaces using contact angle measurements. The results of these measurements allow us to evaluate the effect of ionic strength and pH on the protein adsorption. Additionally, the deposition of fluorescent latex particles (under the diffusion-controlled transport) onto the LSZ monolayer, or onto a part of the monolayer that was preliminary adsorbed on the mica was applied to characterize the LSZ adsorption coverage. It should be mentioned that this type of measurement has not been previously described in the literature.

2. MATERIALS

In our studies, LSZ from chicken egg whites was used. This product was purchased from Sigma (L6876) and used without further purification.

LSZ solutions were prepared by dissolving protein powder in an aqueous solution of NaCl at a controlled ionic strength and pH. The suspension was gently mixed using a magnetic stirrer and filtered through a Millipore GS 0.22 μm filter to eliminate any aggregations and impurities. Protein solutions with concentrations in the range of 500−12000 ppm were used immediately after preparation. The protein concentration in each solution was determined using an automatic digital refractometer, RX 5000CX, which measures the refractive index. The LSZ concentration was independently determined from the absorbance measured using a Shimadzu UV−vis spectrometer, using a quartz cell with a 1 cm path length.

Dynamic surface tension measurements were used to analyze the purity of the LSZ solution, which was determined using the pendant drop shape analysis method. As observed in Figure 1, there was

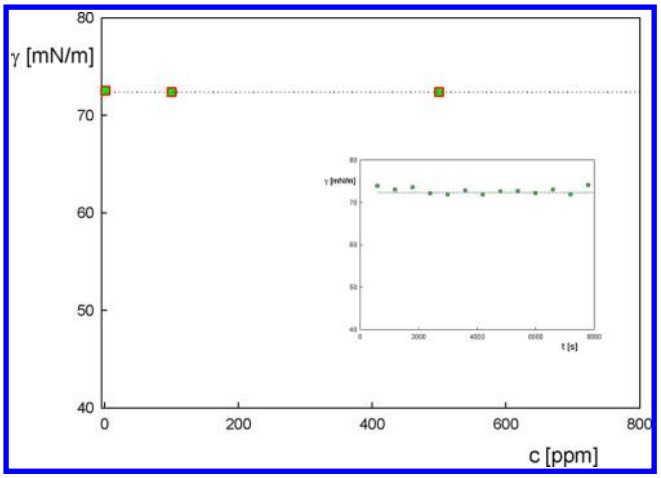

Figure 1. Dependence of the surface tension, γ, on the LSZ concentration. The inset shows the time dependence of the surface tension, $\gamma-t$, for the bulk concentration of 10 ppm LSZ.

practically no change in the surface tension of the 10 ppm LSZ solution over the course of two hours, which is much larger than the typical time required of the DLS and viscosity measurements, that is, 5−10 min. The LSZ solutions with concentrations in the range of 10−1000 ppm exhibited a surface tension of 72.4 ± 0.2 mN/m. This result essentially coincides with the surface tension of triple-distilled water, which was used in our studies.

The pH of the LSZ solutions was experimentally determined to be concentration-dependent (Figure 2). The pH changed from 5.3 for

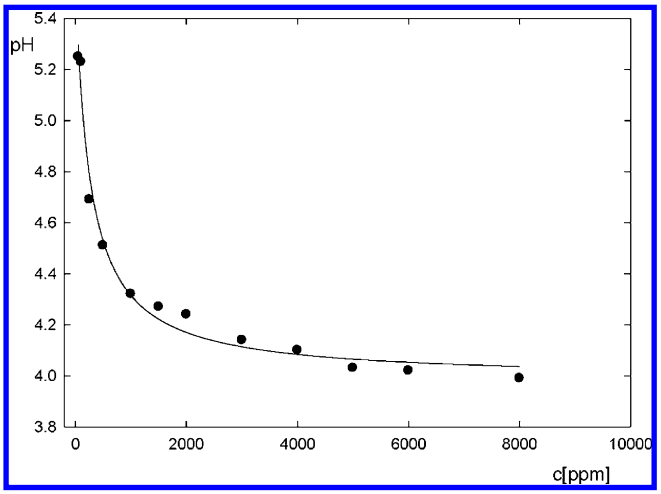

Figure 2. Dependence of the pH values measured in LSZ solutions on the macromolecule concentration at a constant ionic strength of $I = 1 \times 10^{-2}$ M fixed with NaCl.

pure water to 4.0 for the LSZ solution with a concentration of 6000 ppm. Note that near constant pH values were reached within the high concentration ranges of LSZ (3000 ppm).

Fluorescent latex particles were purchased from Duke Scientific Corporation and used without further purification. The size and shape of the particles were analyzed using scanning electron microscopy (SEM; see Figure 3). These measurements were performed using a

dx.doi.org/10.1021/la301558u | Langmuir 2012, 28, 11502−11510

JEOL JSM-3700F field emission scanning electron microscope at an operating voltage of 15 keV.

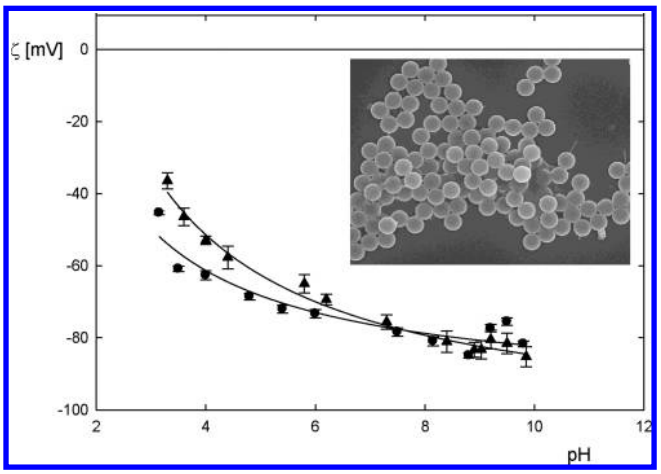

Figure 3. Dependence of the zeta potential, ξ, of the fluorescent latex particles on pH. The marks denote the experimental values determined for the different ionic strengths: ●, $I = 1 \times 10^{-3}$ M; ▲, $I = 1 \times 10^{-2}$ M. The inset shows the SEM image of the fluorescent latex particles.

Deionized water with a conductivity of ca. 0.8 μS/cm was used during the preparation of all solutions. Sodium chloride (NaCl), hydrochloric acid (HCl), and sodium hydroxide (NaOH) were purchased from Aldrich and Sigma. NaCl was used as the supporting electrolyte. All electrolyte solutions were filtered using a 0.22 μm Millipore filter, and all experiments were performed at a constant temperature of 293 ± 0.1 K (20 ± 0.1 °C).

Mica plates from Mica & Micanite Supplies, Ltd., England, were used as the model adsorbent. The sheets were freshly formed before each experiment and used without further pretreatment. The bare mica surface is negatively charged in aqueous solutions, with a charge density of −2.1 e/nm^2.[17] The electrokinetic characteristics of the bare mica surface in the supporting electrolyte solution (NaCl) were determined from streaming potential measurements, such as those described by Scales et al.[18] The zeta potential of the bare mica surface increases monotonically with increasing the ionic strength, reaching −87 mV at $I = 1 \times 10^{-3}$ M and −38 mV at $I = 1 \times 10^{-2}$ M at pH 7.4.

3. METHODS

3.1. Dynamic Light Scattering and Zeta Potential Measurements. The size of the protein molecule was determined using dynamic light scattering (DLS) on a Zetasizer Nano ZS Malvern instrument, which enables measurements within diameter ranges of 0.6 nm to 6 μm. The Nano ZS instrument incorporates noninvasive backscatter (NIBS) optics, which permits measurements of the time-dependent fluctuations in intensity of the scattered light that results from the Brownian motions of the particles/macromolecules. The analysis of the intensity fluctuations enables the determination of the diffusion coefficients of the particles/macromolecules, which are then converted into a size distribution. The diffusion coefficient is calculated from the following time correlation function:

$$g(\tau) = A[1 + B \exp(-2Dq^2\tau)] \quad (1)$$

where D is the diffusion coefficient, τ is the sample time, A is the baseline of the correlation function, B is the intercept of the correlation function, $q = [(4\pi n/\lambda_o)\sin(\theta/2)]$ is the scattering vector, n is the refractive index of the solution, λ_o is the wavelength of the laser, and θ is the scattering angle. The time-dependent autocorrelation function of the photocurrent was acquired every 10 s with 15 acquisitions for each run. The sample solution was illuminated with a 633 nm laser, and an avalanche photodiode was used to measure the intensity of the light scattered at the angle of 173°.

The electrophoretic mobility was measured using the laser Doppler velocimetry (LDV) technique in a Zetasizer Nano ZS within the range of 3 nm to 10 μm. The LDV technique applies a voltage across a pair of electrodes that are placed at both ends of the cell containing the dispersion of particles. The velocity of the charged particles, which are attracted to the oppositely charged electrode, was measured and expressed in units per the field strength as the electrophoretic mobility μ_e,

$$\mu_e = \frac{2\varepsilon\zeta F(\kappa a)}{3\eta} \quad (2)$$

where ε is the dielectric constant of water and $F(\kappa a)$ is the function of the dimensionless parameter κa with $\kappa^{-1} = (\varepsilon kT/2e^2I)^{1/2}$, which represents the double-layer thickness, where e is the elementary charge, k is the Boltzmann constant, T is the absolute temperature; $I = 1/2(\sum_i c_i z_i^2)$ is the ionic strength, where c_i represents the concentration of ions and a is the characteristic dimension of the protein molecule. The electrophoretic mobility was measured at a fixed ionic strength that was regulated by addition of NaCl to levels of $I = 5 \times 10^{-3}$ M, 10^{-2} M, and 0.15 M within pH 3.0−11.0.

3.2. Viscosity Measurements. The dynamic viscosity of the protein solutions was measured using a capillary viscometer equipped with a conductivity sensor, which is in accordance with the previously described procedure.[19] The suspension flow rate (v_{sus}) of a volume of 10 cm^3 through a capillary with an internal diameter, R, was calculated as $\langle V\rangle = v_{sus}/\pi R^2 t$, where t is the time required for the suspension to pass through the capillary. The averaged shear rate ($\langle G\rangle = \langle V\rangle/R$) in the capillary was 1.8×10^{-2} s^{-1}. The device was calibrated using pure liquids of known viscosity, such as water, butyl and amyl alcohols, or ethylene glycol. The precision of the viscosity measurement over the range of 1−10 mPa·s was estimated to be 0.5%. The concentrations of the protein solutions used for the viscosity measurements were changed within the range of 500−12000 ppm. The density of these protein solutions was measured using a pycnometer.

3.3. Contact Angle Measurements. Axisymmetric drop shape analysis (ADSA) was used to measure the contact angle with a high accuracy of 1°. Contact angles were measured by the direct analysis of shape of sessile drops.[20] The protein film, which was first deposited onto mica plates, was dried, and the plate was placed into a thermostatted chamber that was saturated with water vapor to prevent the evaporation of the drops during the measurement. Droplets were created at the tip of a syringe and carefully placed onto the film surface. The volume of the droplets was kept constant at 20 μL. The video image of the sessile drop was transmitted from a charge-coupled device (CCD) video camera to a digital video processor, which performed the frame grabbing and digitization of the image. The Young−Laplace equation was then fitted to the digitized profile of the drop, and the contact angle values were determined by differentiating the fitted equation for the three-phase contact. All contact angle measurements were performed at 293 K.

3.4. Colloid Deposition Measurements. The LSZ adsorption coverage was formed under diffusion-controlled transport conditions. Freshly cleaved mica plates were placed into an LSZ solution to enable adsorption for the fixed times. After the substrate had been covered by the protein, it was then washed with a pure electrolyte solution and immersed into a fluorescent latex suspension. The negatively charged latex particles were deposited from their suspensions of a known density. Subsequently, an optical and fluorescent microscope (Zeiss, Imager Z1m) that was coupled to a CCD camera (AxioCam MRm) was used with image analysis software to determine the surface coverage of the particles.

The average size, R_H, of the negatively charged fluorescent latex particles used in the experiments was 0.40 μm, with a standard deviation of 0.004 μm, at $I = 1 \times 10^{-2}$ M and pH 3.0. The average size, R_H, of the latex particles slightly increased with pH, reaching a value of 0.42 μm at pH 10.0.

The zeta potential of the fluorescent latex particles was determined from microelectrophoresis. Figure 3 demonstrates the pH dependence of the zeta potential at ionic strengths of 1×10^{-3} M and 1×10^{-2} M

dx.doi.org/10.1021/la301558u | Langmuir 2012, 28, 11502−11510

NaCl. It was observed that the zeta potential of the latex particles increased monotonically with pH, from −37 mV at pH 3.5 to −80 mV at pH 7.8, at $I = 1 \times 10^{-2}$ M.

4. RESULTS AND DISCUSSION

The structural properties of LSZ are well-known, including the amino acid sequence and X-ray data for the crystal structure. It is thought that the LSZ molecule has a two-domain structure. In the first domain, the polypeptide chain is folded, forming β-sheets, while the second domain is dominated by the α-helix structure.[21] The presence of four S−S bridges in the LSZ molecule provides its high pH and thermal stability. Polar and nonpolar patches of amino acids are nonuniformly distributed along the surface of the molecule. The conformation of the LSZ is highly stable in the pH range from 4 to 11. The high value of the isoelectric point (iep) found in the pH range of 10−11 is mainly caused by the high pK_a values of Arg (equal to 12.5) and Lys (equal to 10.8). In the native protein, these amino acids are immersed in the hydrophobic environment and are therefore not accessible to water molecules until the pH reaches very high values.

For the quantitative analysis of LSZ adsorption, information on the diffusion coefficient, shape of the molecule, and the effective (uncompensated) charge on its surface are needed. From the DLS measurements, it has been determined that the diffusion coefficient of LSZ was 12.2×10^{-7} cm^2/s (for the concentration range of 100−5000 ppm and ionic strength of I = 0.15 M). Using the experimental value of the LSZ diffusion coefficient, the hydrodynamic radius, R_H, was calculated and found to be 2.0 nm (Figure 4). The LSZ molecule is a spheroid

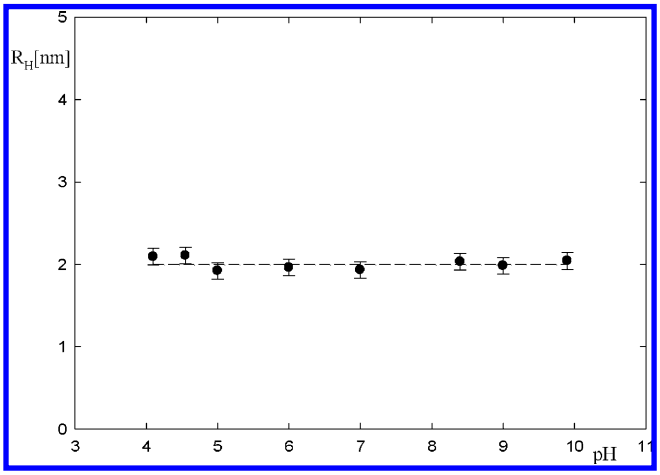

Figure 4. Hydrodynamic radius, R_H, of the LSZ macromolecule, which was determined from the averaged scattering intensity from the DLS method as a function of pH for c = 1500 ppm LSZ and $I = 1 \times 10^{-2}$ M.

with dimensions of 4 nm × 3 nm × 3 nm. Consequently, the nominal aspect ratio, λ (i.e., the ratio of the length to the diameter), is equal to 1.3, which means that the LSZ molecule is slightly elongated.

The molecular volume of the protein, ν_m, can be calculated from the molecular mass, M, as $\nu_m = M/\rho A_v$, where ρ is the protein density and A_v is Avogadro's number. According to this calculation, the ν_m of LSZ is equal to 17.22 nm^3. Alternatively, using the dimensions of the LSZ molecule (4 × 3 × 3 nm^3), one can calculate the molecular volume (assuming its prolate spheroid shape) according to the following formula: $\nu_s = 4\pi a_s^2 b_s/3$ = 18.80 nm^3. It can be observed that the latter value exceeds the previously calculated (17.22 nm^3) molecular mass by approximately 1.1 times. The higher ν_s value suggests a lower density of the LSZ molecule with a void ratio of $1 - (\nu_m/\nu_s)$ = 0.085.

The effective charge of the LSZ molecule in solutions is crucial for interpreting the adsorption and deposition phenomena. The charge can be derived from the electrophoretic mobility, μ_e, measurements. The dependence of μ_e on the pH of LSZ solutions was measured at the three ionic strengths, 10^{-3}, 10^{-2}, and 0.15 M, and these results are shown in Figure 5. For $I = 1 \times 10^{-3}$ M (curve 1), the electrophoretic

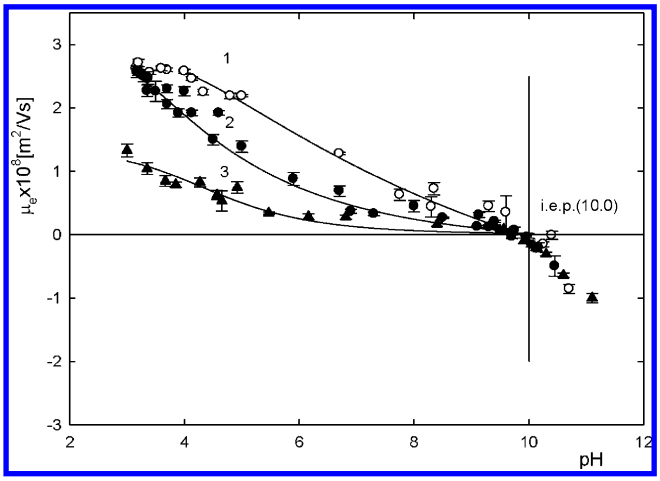

Figure 5. Dependence of the electrophoretic mobility, μ_e, of LSZ on pH. The marks denote the experimental values: curve 1, ○, $I = 1 \times 10^{-3}$ M; curve 2, ●, $I = 1 \times 10^{-2}$ M and curve 3, ▲, I = 0.15 M. The solid lines are obtained by interpolation.

mobility monotonically decreases from 2.8×10^{-8} m^2(V s)$^{-1}$ at pH 3.0 to 0.0 m^2(V s)$^{-1}$ at pH 10.0. The pH value at an electrophoretic mobility equal to zero is usually referred to as the iep. Based on theoretical calculations, the iep of LSZ was predicted to be 9.54, which is slightly smaller than our experimentally determined value at pH 10.0. The latter value of iep, which was also reported by Pan et al.,[22] indicates that the LSZ molecule is positively charged in the pH range from 3.0 to 10.0.

The effective (uncompensated) charge of the LSZ molecules, q, can be calculated from the electrophoretic mobility μ_e and hydrodynamic radius $R_H = kT/6\pi\eta D$ using the Lorenz−Stokes equation, which is derived in ref 19:

$$q = \frac{\langle U \rangle}{\langle M \rangle E} = \frac{kT}{D}\mu_e = 6\pi\eta R_H \mu_e \quad (3)$$

where $\mu_e = \langle U \rangle / E$ and $\langle U \rangle$ is the averaged migration velocity of the protein molecule in a uniform electric field E, $\langle M \rangle$ is the average mobility, D is the diffusion coefficient, and η is the dynamic viscosity of water. Considering that $e = 1.602 \times 10^{-19}$ C, eq 3 can be used to calculate the average number of elementary charges per molecule, N_c:

$$N_c = \frac{6\pi\eta R_H}{e}\mu_e \quad (4)$$

By substituting our experimental data into eq 4, we obtained the results presented in Figure 6. The effective charge decreases with pH and the ionic strength. In Figure 6, the experimental data are compared with the theoretical prediction by

dx.doi.org/10.1021/la301558u | Langmuir 2012, 28, 11502−11510

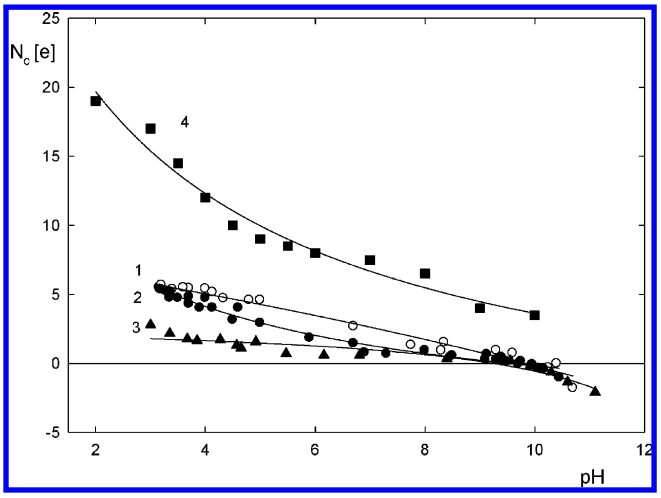

Figure 6. Number of uncompensated charges, N_c, of LSZ molecules as a function of pH at different ionic strengths: ○, $I = 1 \times 10^{-3}$ M; ●, $I = 1 \times 10^{-2}$ M and ▲, $I = 0.15$ M. The values were determined as $N_c = (6\pi\eta R_H)/(e)\mu_e$ and are compared with ■, the theoretical total charge of the LSZ molecule, as calculated by Ernkowa.[23]

Ernkowa,[23] who evaluated the dependence of the total charge of LSZ on the pH. Our values are much smaller, indicating that 20−30% of the nominal charge is present on surface of the LSZ molecule. The effect of lowering the surface charge with by increasing the ionic strength can be explained by the coadsorption of the counterions (Cl^- in our case), which is often referred to as the ion condensation phenomenon.[24]

As previously demonstrated for BSA,[25] additional information on the protein suspensions and their degree of aggregation can be derived from measurements of the dynamic viscosity, which were performed using low values of the volume fraction. The dependence of the relative viscosity, η/η_s, of a suspension (where η is the suspension viscosity and η_s is the solvent viscosity) on its volume fraction, Φ_V, is quantitatively related to the shape of the molecule or its aggregate. For rigid and spherical particles, the Einstein model predicts the following:

$$\frac{\eta}{\eta_s} = 1 + 2.5\Phi_V \tag{5}$$

For nonrigid and nonspherical particles, eq 5 can be written as:

$$\frac{\eta}{\eta_s} = 1 + \nu\Phi_V \tag{6}$$

where ν is the viscosity increment, also known as the Simha factor, which is related to the intrinsic viscosity, $[\eta]$, defined as:

$$[\eta]_\Phi = \lim_{\Phi\to 0}\left(\frac{\eta - \eta_s}{\eta_s\Phi}\right) = \nu \tag{7}$$

The viscosity increment, ν, is referred to as the "universal shape function", which is directly related to shape of the particle. If a macromolecule carries multiple charges, the electrostatic charge can also affect the intrinsic viscosity of its solution. Three types of electro-viscous contributions can be distinguished for polymers in solution: (1) the primary effects due to the resistance of the diffusive double layer that surrounds the molecule; (2) the secondary effects arising from the repulsion between the double layers formed at the macromolecule surface; and (3) the tertiary effects arising from the interparticle repulsion that affects the shape of the macromolecules.

The relative viscosity of the LSZ solutions, η/η_s, in a range of $\Phi_V < 0.009$ is illustrated in Figure 7. Our experimental results

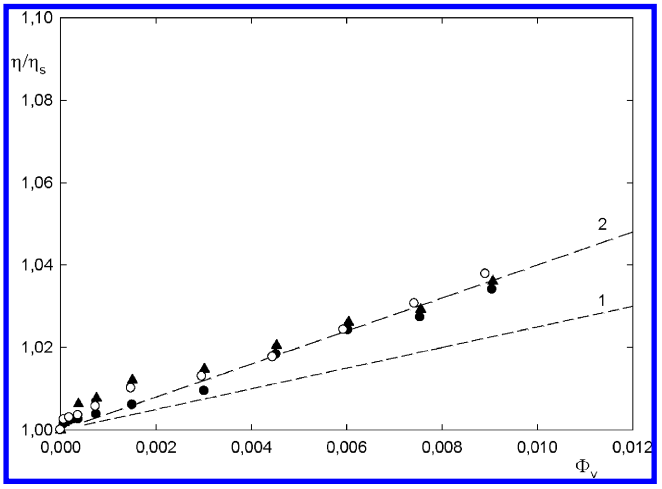

Figure 7. Dependence of the relative viscosity of the LSZ solutions, η/η_s, on the volume fraction, Φ_V, determined for $T = 298$ K at two ionic strengths, i.e., $I = 0.15$ M at the various pHs (●, pH = 6.5; ▲, pH = 9.5) and $I = 1 \times 10^{-2}$ M at pH = 6.5 (○). Dashed line 2 denotes the linear fit of a slope equal to 4.0, and line 1 denotes the linear fit of a slope equal to 2.5.

of the viscosity at two ionic strengths, that is, $I = 0.15$ M (at pH of 6.5 and 9.5) and $I = 1 \times 10^{-2}$ M (at pH 6.5), are fairly well-described by a linear dependence with a slope equal to 4.0. The correction for hydration effects leads to the apparent volume increase of LSZ, which results in a lower slope of 3.0 (for $[\eta]_c = 0.75[\eta]$). The intrinsic viscosity, $[\eta]$, values are similar to the theoretical values predicted for a bare molecule. Using the method that has previously applied to polyelectrolytes,[19] one can calculate the effective length, L_e, of the molecule from the formula: $L_e^* = (4\nu^*\lambda_c^2/\pi)^{1/3}$, where λ_c was calculated using the experimental values of the intrinsic viscosity, $\nu_m^* = \nu_m(d_h/d_c)^2$. In electrolyte solutions, LSZ molecules, similar to most proteins, are strongly hydrated, indicating that their effective diameter, and consequently the aspect ratio, becomes slightly larger. Assuming that, on average, one monolayer of water dipoles (with a diameter of 0.145 nm) is uniformly bound to the LSZ molecule, one can calculate that the diameter of hydrated LSZ molecule is $d_h = 3.29$ nm, and the effective aspect ratio, λ^*, is equal to 1.3.[26] Using this assumption, it was found that $L_{ef} = 5.6$ nm, which is larger than the nominal length of LSZ in the crystalline state, where it is equal to 4.0 nm.

It is reported in the literature[27] that, at a relatively low concentration of LSZ, the molecule exists mostly in form of monomers and dimers, whereas at higher concentrations, large LSZ clusters dominate and are in dynamic equilibrium. Kim et al.[13] who adsorbed LSZ molecules on a mica surface observed LSZ clusters comprised of approximately five molecules per cluster.

To verify that LSZ is a cationic protein under a wide range of conditions, we investigated the wetting properties of the LSZ films (in the range of monolayers) on mica by measuring the contact angles. The effect of ionic strength and pH on the protein adsorption was evaluated using these measurements. The adsorption process was performed with LSZ solutions at two ionic strengths, 1×10^{-2} M and 0.15 M, and at two different pH values, 4.0 and 7.0. A mica plate was immersed in

dx.doi.org/10.1021/la301558u | Langmuir 2012, 28, 11502−11510

the LSZ solution at a fixed pH for 5 min and then washed with water of the same pH and finally dried with nitrogen. The measured contact angle for the bare mica surface is relatively low, that is, less than 10°. We examined the contact angle with the respect to its change both with the adsorption time and LSZ concentration. The measured contact angle values are plotted against the adsorption time for two LSZ concentrations in Figure 8. The dotted line drawn in Figure 8 at the ordinate of

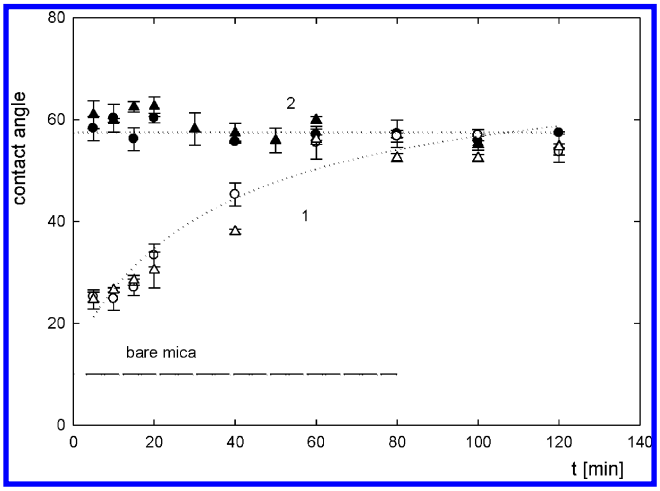

Figure 8. Dependence of the contact angle measured on mica covered with a fraction of LSZ monolayer as a function of the adsorption time. The adsorption occurred from solutions of two different LSZ concentrations, two pH values and at an ionic strength of $I = 1 \times 10^{-2}$; curve 1, $c = 0.5$ ppm LSZ (●, pH = 4.0 and ○, pH = 7.0); curve 2, $c = 5$ ppm LSZ (■, pH = 4.0 and □, pH = 7.0).

10° presents the average value of the contact angle measured for water droplets resting on the bare mica surface, that is, when no adsorbed LSZ molecules are present. As observed in Figure 8, the contact angle on mica that was preliminary subjected to adsorption from the 0.5 ppm LSZ solution rises steeply with the adsorption time, from 10° to approximately 57.5°, reaching the plateau value for the 60 min adsorption time (curve 1). However, when the LSZ adsorption occurred from the LSZ solution with a concentration of 5 ppm, the practically constant contact angle was measured within the measurement accuracy, independently of the adsorption time, two hours (curve 2). These results suggest that 5 min of adsorption time at an LSZ concentration of 5 ppm assures surface coverage that produces the plateau value of the contact angle. However, at the lowest LSZ concentration (0.5 ppm), a much lower adsorption coverage that depended on the adsorption time was formed.

In the case of the adsorption rate that is limited by the diffusion transport, the surface coverage can be calculated from the following equation: $\Theta_{diff} = 2n_bS(Dt/\pi)^{1/2}$, where n_b is the number of macromolecules in the solution bulk, S is the area occupied by the adsorbed macromolecule ($S = 12.56 \times 10^{-14}$ cm^2), and t is the adsorption time. However, we should remember that the adsorption surface coverage increases linearly with the square of root of time only for low coverage. For higher adsorption coverage blocking effects become significant. The maximum coverage can be predicted by Monte Carlo simulation performed according to RSA models.

When we calculated the surface coverage from the above-mentioned equation, we obtained $\Theta = 0.5$ for LSZ concentrations of 5 ppm after 5 min of adsorption time, but after the same adsorption time from LSZ solutions with a concentration of 0.5 ppm, the coverage is only $\Theta = 0.05$. The coverage calculated for the lower LSZ concentration (0.5 ppm) after an adsorption time of 60 min results in $\Theta = 0.2$ and shows that this value sufficient to ensure the maximum contact angle value.

For the LSZ concentration of 10 ppm, we performed a series of experiments to examine the dependence of the contact angle on pH and the ionic strength. These results are presented in Figure 9. For an ionic strength of $I = 1 \times 10^{-2}$ M, the contact

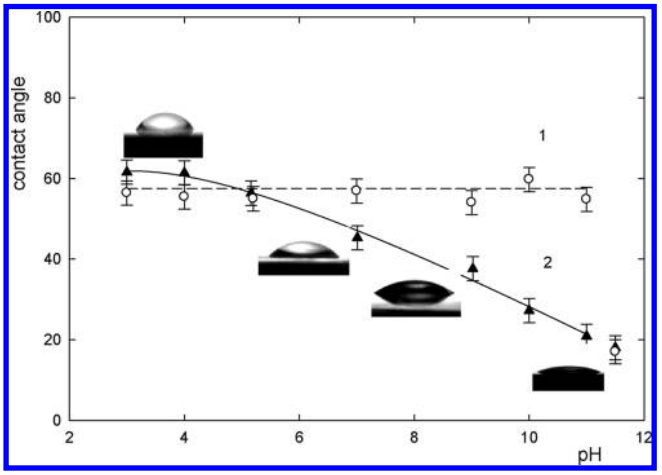

Figure 9. Measured contact angle values on mica covered with a fraction of LSZ monolayer formed under variable pH. The adsorption occurred during $t = 5$ min from an LSZ solution of $c = 10$ ppm at two ionic strengths: curve 1, ○, $I = 1 \times 10^{-2}$ M and curve 2, ▲, $I = 0.15$ M. The lines are obtained by interpolation.

angle approaches the limiting value equal to 57.5°, which remains constant in the pH range of 3−11 but falls at pH = 11.5 to a value of 18° (curve 1 in Figure 9). However, the LSZ adsorption at the higher ionic strength, $I = 0.15$ M, results in the contact angle decreasing with pH, from 57.5° at pH 3.0 to 18° at a relatively high pH of 11.5 (curve 2 in Figure 9). Based on our earlier evaluations, we proposed that for the ionic strength of $I = 0.15$, in the pH range above 5.5, the surface coverage starts to decline to $\Theta = 0.2$. It is worth emphasizing that the lower contact angles are produced when the LSZ adsorption on mica occurs at higher ionic strength, 0.15 M, which is in accordance with lowering the zeta potential of LSZ molecules by increasing the ionic strength (c.f., Figure 10). Note that the larger positive zeta potential of the LSZ molecules results in higher measured contact angles on mica covered with the adsorption film, which indicates that the adsorption is driven by electrostatic interactions of the opposite charges of the adsorbate and the adsorbent.

The effect of the ionic strength and the surface charge on the adsorption of LSZ on a PEGylated surface was systematically studied by Pasche et al.[14] These authors conclude that the adsorption of hard, charged proteins, such as LSZ, is electrostatically driven.

The decrease of the contact angle with pH can be explained by a decrease in the attractive forces between the positively charged LSZ and the negatively charged mica. To explain these results, we compared the zeta potential of the mica surface and the LSZ molecule in Figure 10. In the pH range between 4.0 and 10.0, the zeta potential, ζ, of mica at an ionic strength of 1×10^{-2} M is approximately −60 mV.[28] Under the same

dx.doi.org/10.1021/la301558u | Langmuir 2012, 28, 11502−11510

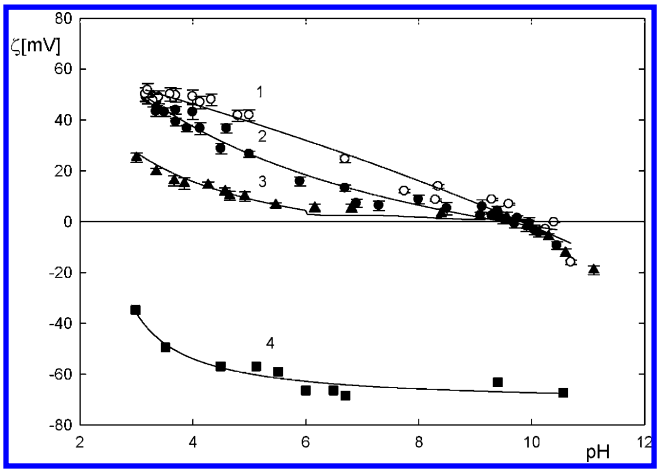

Figure 10. Dependence of the zeta potential of the LSZ macromolecule (curves 1–3) on the pH. The marks denote the experimental values determined from the DLS results for curve 1, ○, $I = 1 \times 10^{-3}$ M; curve 2, ●, $I = 1 \times 10^{-2}$ M and curve 3, ▲, $I = 0.15$ M. Curve 4, ■, denotes the dependence of the mica zeta potential on the pH, as determined by the streaming potential measurements.[28].

conditions, the zeta potential, ζ, of the LSZ molecule varies from 40 mV to 0 mV, reaching the lowest value at a pH of 10.0. In fact, the electrostatic interactions decrease with increasing pH. When the ionic strength increases to the higher value (0.15 M), and consequently, screening the surface charges by the electrolyte becomes more effective, the attractive interactions between LSZ and mica diminish, mainly resulting from the diminished LSZ charge, which results in lower surface coverage. However, the contact angle measurements suggest that the coverage remains significant at pH = 10.0, at which the surface of the LSZ molecule is neutral or only contains a small positive charge. This observation indicates that nonelectrostatic (specific) forces also contribute to the adsorption. These additional forces likely originate from van der Waals interactions and hydrogen bonding between the amine groups of the LSZ molecule with silanol groups formed on mica in contact with water. Additionally, even if the surface amino acid net charge would be neutral, the acid may be situated within a local domain of a net-positive charge. Our results show that the wettability/hydrophobicity of mica is extremely sensitive to the presence of a fraction of monolayer of the adsorbed protein at the mica–solution interface. Rendering a solid surface hydrophobic by adsorption is relatively simple compared with other methods (e.g., AFM), which are inconvenient and time-consuming.

Hartvig[29] performed interesting theoretical calculations that indicated that the adsorption of LSZ on a charged surface occurs as a result of the electrostatic interactions that are dependent on the interfacial charges modified by pH and on the presence of electrolytes. These authors calculated that the change in the surface potential following the adsorption of LSZ on mica (i.e., an increase from a more negative potential, similar to that of bare mica surface, to a less negative or even slightly positive value) has contributions from two effects: (i) the rise of pH at the interface due to the protein adsorption and (ii) the adsorption-induced neutralization of the surface potential. The complex adsorption behavior of LSZ on a charged surface can be explained by assuming pH regulation of the charge of amino acid residues of the adsorbing protein.

To examine the homogeneity of the LSZ adsorption coverage on mica, additional experiments were performed with respect to the probing deposition of negatively charged fluorescent latex particles on the mica surfaces that were preliminary modified by the adsorption of LSZ at different pH values. A fluorescence microscope was used to visualize the micrometer-scale latex particles immobilized by the previously adsorbed protein nanoparticles; these results are presented in Figure 11. Investigations such as these appear to be a promising tool for investigating the proliferation of cells or cell differentiation on a surface.

A series of micrographs of the latex particles adsorbed onto the LSZ monolayer fraction at the various pHs are shown in Figure 11. The adsorption of LSZ was performed under diffusion-controlled transport conditions using the following conditions: $c = 10$ ppm LSZ ($n_b = 43.0 \times 10^{13}$ particle/cm^3), $I = 1 \times 10^{-2}$ M, and the adsorption time $t = 5$ min. We examined the ability of the adsorbed films to capture the latex particles under these conditions, at which the surface coverage of LSZ approached the monolayer. For these experiments, the freshly cleaved mica plates were placed into a 10-ppm LSZ solution for a fixed time of adsorption, $t = 5$ min. The adsorption occurred at the different pH values ranging from 3.0 to 11.0. The substrate covered by the protein monolayer was then washed with the pure NaCl electrolyte solution of the same pH and then immersed into the fluorescent latex suspension corresponding to $n_b = 5.3 \times 10^8$ particles/cm^3 at an ionic strength of 1×10^{-2} M for $t = 30$ min.

As observed in Figures 11a–e, the fluorescent latex particles are randomly distributed on the surface. The dimensionless surface coverage of the fluorescent latex particles was calculated from the following equation: $\Theta_p = \pi a_p^2 N_p / S_c$, where a_p is the radius of the latex particles, N_p is the number of adsorbed particles, and S_c is the surface area. These experiments demonstrate that the LSZ coverage on mica had to be strongly pH-dependent. The coverage of the latex particles decreases from $\Theta = 0.05$ at pH 5.3 (Figure 11a) to $\Theta = 0.001$ at pH 11.0 (Figure 11e). The latex coverage formed after the adsorption of LSZ at pH= 5.3 approaches half of the limiting value obtainable for a homogeneous surface.

The latex deposition experiments on the bare mica surface show that no measurable deposition of these microparticles occurred when there were no preadsorbed LSZ molecules present. However, the latex fluorescent particles were captured when the LSZ coverage, $\theta_{ls,z}$, was higher than the critical coverage. For the high LSZ coverage range, fluctuations in the distribution of LSZ molecules along the mica surface (resulting in fluctuations of the local surface charge) have no influence on the distribution of the captured latex particles because their cross-sectional area is 17.77×10^3 times larger than that of the LSZ molecule cross-sectional area. For the above analyses, immobilization of the latex particles on the centers consisting of a single LSZ molecule is not possible due to the low attraction energy. Therefore, capture of the latex particles should occur at the adsorption centers that are composed of a few closely situated LSZ molecules. There are two possible reasons for the observed phenomena: (1) the diminishing adsorption of LSZ with increasing pH and (2) changes in the electrostatic interactions between the negatively charged latex particles and the positively charged LSZ monolayer. Given that at an ionic strength of 1×10^{-2} M, the contact angle does not change with pH, regardless of the LSZ concentration (c.f., Figures 9–10), one may conclude that under these conditions the electrostatic

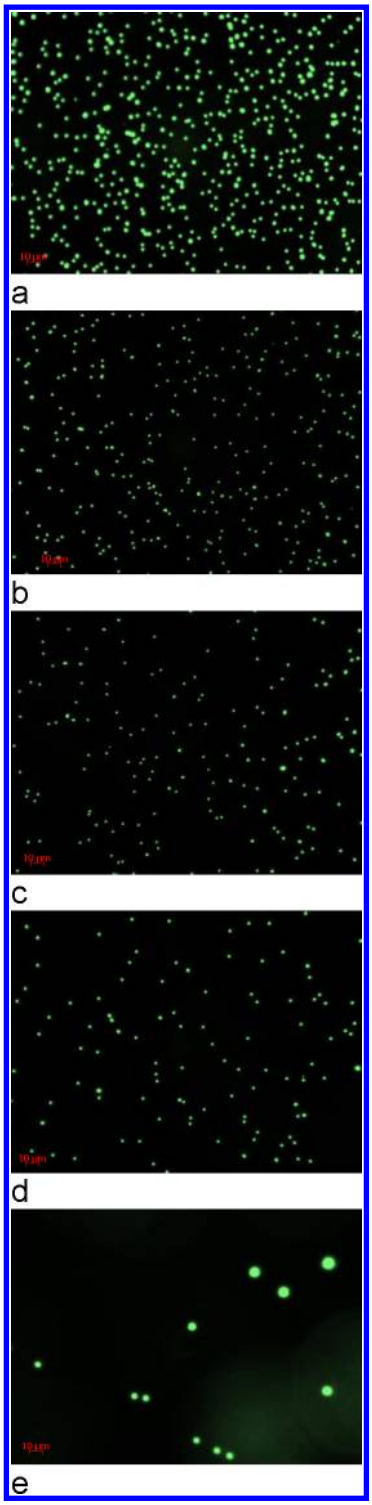

Figure 11. Micrographs obtained from fluorescence microscopy measurements of the negatively charged latex particles that were deposited on mica that had been previously covered with a fraction of LSZ monolayer adsorbed during t = 5 min from a solution of c = 10 ppm LSZ at $I = 1 \times 10^{-2}$ M NaCl and at variable pH values: (a) pH = 5.3, (b) pH = 7.0, (c) pH = 9.0, (d) pH = 10.0, and (e) pH = 11.0.

interactions between mica and LSZ are strong enough for the monolayer adsorption. However, the charge density of the LSZ monolayer strongly depends on the pH, which determines the contact angle dependence on the pH. Finally, it is interesting to note that a similar behavior was previously observed for a heterogeneous surface modified by controlled adsorption, as described by Zhang et al.[30] These authors demonstrated that the negative surface containing cationic nanoparticles captures and holds negative silica microparticles.

5. CONCLUSIONS

The complementary properties of LSZ molecules in the solution bulk and at the mica−solution interface were investigated. The dynamic viscosity measurements were performed to determine the LSZ dimension in solution. The dynamic viscosity data were converted to the effective length (L_{ef}) of the molecule, which was found to be L_{ef} = 5.6 nm. The electrophoretic measurements performed at various pH values and ionic strengths allowed us to directly determine the number of uncompensated (electrokinetic) charges on LSZ molecules at various solution compositions. This charge was found to be considerably smaller than the theoretically predicted value.

The combination of the determined parameters provides insight into the structure and properties of the protein monolayer adsorbed onto the mica surface at various pH values. We observed that the hydrophobicity/wettability of the mica surface modified by low concentrations of LSZ exhibits a very strong dependence on both the pH and the ionic strength. The highest contact angle was measured on mica modified by LSZ adsorption coverage and was found to be equal to $0.2 < \Theta < 0.5$. The coverage in this range was formed under the conditions at which the protein molecule possesses the greatest charge, fine-tuned by the lowest pH = 3. In the pH range in which the protein possesses a weak negative charge (at pH 11), the lowest contact angle was measured. The combined zeta potential and the contact angle measurements show that the adsorption is primarily driven by electrostatic interactions between the oppositely charged protein (positive) and the support (negative). A similar process also occurs for the deposition of negatively charged latex particles onto surface of mica, which was first modified by LSZ adsorption to render the mica positively charged.

AUTHOR INFORMATION

Corresponding Author

*E-mail: ncjachim@cyf-kr.edu.pl.

Notes

The authors declare no competing financial interest.

ACKNOWLEDGMENTS

This work was supported by Grant MNiSzW N204 028536.

REFERENCES

(1) Su, T. J.; Lu, J. R. The Effect of Solution pH on the Structure of Lysozyme Layers Adsorbed at the Silica-Water Interface Studied by Neutron Refletion. *Langmuir* **1998**, *14*, 438−445.

(2) Lu, J. R.; Swann, M. J.; Peel, L. L.; Freeman, N. J. Lysozyme Adsorption Studies at the Silica/Water Interface Using Dual Polarizaion Interferometry. *Langmuir* **2004**, *20*, 1827−1832.

(3) Robeson, J. L.; Tilton, R. D. Spontaneous Reconfiguration of Adsorbed Lysozyme Layers observed by Total Internal Reflection Fluorescence with pH-sensitive Fluorophore. *Langmuir* **1996**, *12*, 6104−6113.

(4) Daly, S. M.; Przybycien, T. M.; Tilton, R. D. Coverage-Dependent Orientation of Lysozyme Adsorbed on Silica. *Langmuir* **2003**, *19*, 3848−3857.

(5) Wertz, C. F.; Santore, M. M. Adsorption and Reorientation Kinetics of Lysozyme on Hydrophobic Surfaces. *Langmuir* **2002**, *18*, 1190−1199.
(6) Felsovalyi, F.; Mangiagalli, P.; Bureau, C.; Kumar, S. K.; Banta, S. Reversibility of the Adsorption of Lysozyme on Silica. *Langmuir* **2011**, *27*, 11873−11882.
(7) Fears, K. P.; Sivaraman, B.; Powell, G. L.; Wu, Y.; Latour, R. A. Probing the Conformation and Orientation of Adsorbed Enzymes Using Side-Chain Modification. *Langmuir* **2009**, *25* (16), 9319−9327.
(8) Etheve, J.; Dejardin, P. Adsorption Kinetics of Lysozyme on Silica at pH 7.4: Correlation between Streaming Potential and Adsorbed Amount. *Langmuir* **2002**, *18*, 1777−1785.
(9) Norde, W.; Anusiem, A. C. I. Adsorption, desorption and re-adsorption of proteins on solid surfaces. *Colloids Surf.* **1992**, *66*, 73−80.
(10) van der Veen, M.; Stuart, M. C.; Norde, W. Spreading of proteins and its effect on adsorption and desorption kinetics. *Colloids Surf.* **2007**, *54*, 136−142.
(11) van der Veen, M.; Norde, W.; Stuart, M. C. Electrostatic interactions in protein adsorption probed by comparing lysozyme and succinylated lysozyme. *Colloids Surf.* **2004**, *35*, 33−40.
(12) Blomberg, E.; Claesson, P. M.; Froberg, J. C.; Tilton, R. D. Interaction between adsorbed Layers of Lysozyme Studied with the Surface Force Technique. *Langmuir* **1994**, *10*, 2325−2334.
(13) Kim, D. T.; Blanch, H. W.; Radke, C. J. Direct Imaging of Lysozyme Adsorption onto Mica by Atomic Force Microscopy. *Langmuir* **2002**, *18*, 5841−5850.
(14) Pasche, S.; Voros, J.; Griesser, H. J.; Spencer, N. D.; Textor, M. Effect of Ionic Strength and Syrface Charge on Protein Adsorption st PEGylated Surfaces. *J. Phys. Chem. B* **2005**, *109*, 17545−17552.
(15) Carlsson, F.; Hyltner, E.; Arnerbrant, T.; Malmsten, M.; Linse, P. Lysozyme Adsorption to Charged Surfaces. A Monte Carlo Study. *J. Phys. Chem. B* **2004**, *108*, 9871−9881.
(16) Jachimska, B.; Pajor, A. Physico-chemical characterization of bovine serum albumin in solution and as deposited on surfaces. *Bioelectrochemistry* **2011**, DOI: 10.1016/ j.bioelectroch. 2011.009.004.
(17) Rojas, O. Adsorption of polyelectrolyte on mica. In *Encyclopedia of Surface and Colloid Science*; Marcel Dekker: New York, 2002; p 517.
(18) Scales, P. J.; Grieser, F.; Healy, T. W.; White, L. R.; Chan, D. Y. C. Electrokinetics of the silica-solution interface: a flat plate streaming potential study. *Langmuir* **1992**, *8*, 965.
(19) Jachimska, B.; Jasiński, T.; Warszyński, P.; Adamczyk, Z. Structure of polyallylamine hydrochloride (PAH) in electrolyte solutions: theoretical modeling and measurements. *Colloids Surf., A* **2010**, *355*, 7−15.
(20) Kolasińska, M.; Warszyński, P. The effect of nature of polyions and treatment after deposition on wetting characteristics of polyelectrolyte multilayers. *Appl. Surf. Sci.* **2005**, *252*, 759−763.
(21) RCSB Protein Data Bank. http://www.rcsb.org.
(22) Pan, X.; Yu, S.; Yao, P.; Shao, Z. Self-assembly of β-casein and lysozyme. *J. Colloid Interface Sci.* **2007**, *316*, 405−412.
(23) Ermkowa, E. Lysozyme dimerization: Brownian dynamics simulation. *J. Mol. Model.* **2005**, *12*, 34−41.
(24) Manning, G. S. Limiting Laws and Counterion Condensation in Polyelectrolyte Solutions I. Colligative Properties. *J. Chem. Phys.* **1969**, *51* (3), 924.
(25) Jachimska, B.; Wasilewska, M.; Adamczyk, Z. Characterization of globular protein solusions by dynamic light scattering, electrophoretic mobility and viscosity measurements. *Langmuir* **2008**, *24* (13), 6866−6872.
(26) de la Torre, G. J. Hydration from hydrodynamics. General considerations and applications of bead modeling to globular proteins. *Biophys. Chem.* **2001**, *93*, 159−170.
(27) Stradner, A.; Cardinaux, F.; Schurtenberger, P. A small angle scattering study on equilibrium clusters in lysozyme solutions. *J. Phys. Chem. B* **2006**, *110*, 21222−21231.
(28) Wasilewska, M.; Adamczyk, Z. Fibrinogen adsorption on mica studied by AFM and in situ streaming potential measurements. *Langmuir* **2011**, *27*, 686−696.
(29) Harding, S. E. On the hydrodynamic analysis of macromolecular conformation. *Biophys. Chem.* **1995**, *55*, 69−93.
(30) Zhang, J.; Srivastava, S.; Duffadar, R.; Davis, J. M.; Rotello, V. M.; Santore, M. M. Manipulating microparticles with single surface-immobilized nanoparticles. *Langmuir* **2008**, *24*, 6404−6408.